

## Electron correlations in cross sections for ionization of heliumlike ions by high-energy particle impact

A. I. Mikhailov,<sup>1,2</sup> A. V. Nefiodov,<sup>1,2,\*</sup> and G. Plunien<sup>3</sup>

<sup>1</sup>*Petersburg Nuclear Physics Institute, 188300 Gatchina, St. Petersburg, Russia*

<sup>2</sup>*Max-Planck-Institut für Physik komplexer Systeme, D-01187 Dresden, Germany*

<sup>3</sup>*Institut für Theoretische Physik, Technische Universität Dresden, D-01062 Dresden, Germany*

(Received 20 December 2012; published 8 March 2013)

We have evaluated the dominant contribution of the electron correlations to the single  $K$ -shell ionization cross section of heliumlike atomic systems by impact of high-energy electrons. This study is performed consistently within the framework of nonrelativistic perturbation theory. The results obtained are also applicable for the case of high-energy collisions with arbitrary charged particles whose mass is much less than that of the target. The formula for cross section is represented in the form of a universal scaling. A comparison of our numerical calculations with available experimental data is made.

DOI: [10.1103/PhysRevA.87.032705](https://doi.org/10.1103/PhysRevA.87.032705)

PACS number(s): 34.80.Dp, 34.10.+x

### I. INTRODUCTION

The single ionization of inner-shell electrons by the electron impact is one of the fundamental processes which still attracts considerable interest in collision theory, experimental measurements, and various applications [1–7]. To describe the ionization cross sections, one usually employs either sophisticated numerical approaches or empirical and semiempirical fitting formulas. Significant efforts have been also devoted to investigations of the scaling behavior of ionization cross sections with respect to the incident electron energy [8–13]. However, a consistent theoretical consideration of the problem, which would allow one to deduce the universal scaling laws accurately describing the ionization processes for different atomic targets within the wide energy range from the ionization threshold to asymptotic high energies, is still absent in the literature.

The aim of this paper is to study the universal scalings for weakly bound two-electron targets, which can be obtained within the framework of nonrelativistic perturbation theory. We start with the approximation of noninteracting electrons, which employs the complete basis set of the Coulomb wave functions for the discrete and continuous spectra (Furry picture). In the nonrelativistic problem, the strength of the electron-nucleus interaction is characterized by the small parameter  $\alpha Z \ll 1$ , where  $\alpha$  is the fine-structure constant and  $Z$  is the nuclear charge. In particular, the characteristic velocity of a bound inner-shell electron is  $\alpha Zc$ , where  $c$  is the speed of light. In the following, we shall use the relativistic units ( $\hbar = 1$ ,  $c = 1$ ), which significantly simplify all formulas. A  $K$ -shell electron is also characterized by the averaged momentum  $\eta = m\alpha Z$  and the energy  $E_{1s} = -I$ , where  $m$  is the electron mass and  $I = m(\alpha Z)^2/2$  is the ionization potential. The electron-electron interaction is treated within the framework of perturbation theory, which appears as a series expansion with respect to the small parameter  $1/Z \ll 1$ . The latter represents the ratio of the strength of the electron-electron interaction to the electron-nucleus one. Obviously, the highest accuracy of theoretical predictions, which are obtained to leading

orders of perturbation theory with respect to parameters  $\alpha Z$  and  $1/Z$ , can be achieved for atomic targets with moderate values of  $Z$ . The generalization of the results to the case of heavier targets and relativistic energies requires accounting for the relativistic corrections over the parameter  $\alpha Z$  (see, for example, Refs. [14–18]). The extension of the formulas to the case of light targets requires accounting for the correlation corrections over the parameter  $1/Z$  [19,20].

Let us assume that the incident electron has the energy  $E_p = p^2/(2m)$  and the momentum  $\mathbf{p} = m\mathbf{v}$  at infinitely large distances from the nucleus. To study the universal scalings, it is natural to introduce the dimensionless quantities. For incident electrons, these are the dimensionless momentum  $k = p/\eta = v/(\alpha Z)$  and energy  $\varepsilon = E_p/I = v^2/(\alpha Z)^2$ , which are related to the dimensionless velocity of the projectile calibrated in units of the averaged velocity of a  $K$ -shell electron. Note that the quantity  $\xi = 1/k$  is Sommerfeld's parameter. In ionization processes, it is also convenient to distinguish between the near-threshold ( $\xi \gtrsim 1$ ) and high-energy ( $\xi \ll 1$ ) ranges. The theoretical description near the ionization threshold is always a complicated technical problem since it requires consistently accounting for all bindings in the colliding system. At high energies, the theoretical description is simplified since some bindings become unimportant and therefore can be neglected due to the additional small parameter  $\xi \ll 1$ .

For hydrogenlike ions characterized by small parameters  $\alpha Z$  and  $1/Z$ , the  $K$ -shell ionization cross section deduced to leading order of the perturbation theory can be cast in the following form:

$$\sigma_{1s}^+ = \frac{\sigma_0}{Z^4} Q_{1s}(\varepsilon), \quad (1)$$

where  $\sigma_0 = \pi a_0^2 = 87.974$  Mb and  $a_0 = 1/(m\alpha)$  is the Bohr radius. The universal function  $Q_{1s}(\varepsilon)$  does not depend explicitly on the value of  $Z$ . In Fig. 1, we present two theoretical curves for the function  $Q_{1s}(\varepsilon)$ . In the first calculation, which is justified for high-energy electron impact ( $\varepsilon \gg 1$ ), the incident and scattered electrons are described by the plane waves (Born approximation). The atomic electrons (bound and ionized ones) are described by the Coulomb wave functions, which accurately take into account the electron-nucleus interactions.

\*anef@thd.pnpi.spb.ru

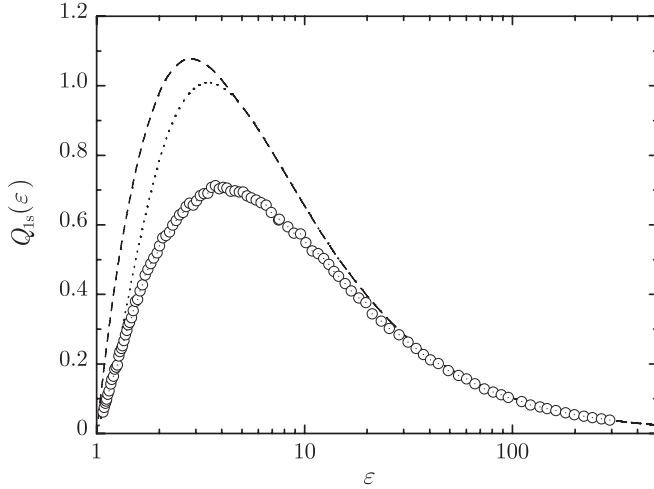


FIG. 1. The universal function  $Q_{1s}(\epsilon)$  dependent on the dimensionless energy  $\epsilon$  of the incident electron. Dotted line, calculation within the Born approximation; dashed line, exact calculation with the Coulomb wave functions. Experimental data: H atom (circles with dots) [25].

In fact, this curve appears from the energy distribution obtained by Bethe in analytical form for the case of the hydrogen atom [21–24]. The second calculation is performed by using the Coulomb wave functions for all electrons involved in the ionization process [24]. This result is justified for arbitrary nonrelativistic energies  $1 \leq \epsilon \ll 2(\alpha Z)^{-2}$ , including the near-threshold range. As can be seen, for the total cross section (1), the near-threshold and high-energy domains match each other already at about  $\epsilon \gtrsim 5$ . In the Born approximation, the cross section is underestimated near the threshold.

In order to test the accuracy of the theoretical results, we compare them with measurements made on hydrogen atoms [25], where the perturbation theory is formally not applicable since the parameter  $1/Z = 1$  is not small. Surprisingly enough, the cross section calculated to leading order reproduces the correct order of magnitude. The disagreement between theory and experiment reaches about 40% at most. The discrepancy is due to two- and three-photon exchange corrections, which are omitted in the theoretical calculations. At  $\epsilon \gtrsim 20$ , cross section (1) already has true asymptotic behavior; that is, the higher-order correlation corrections are small at the high-energy regime. However, this is an exceptional peculiarity of hydrogenlike atomic systems since in such targets there is one slow electron only.

In the case of heliumlike ions being in the ground state, the single ionization cross section obtained to leading order of perturbation theory reads

$$\sigma^+ = 2\sigma_{1s}^+, \quad (2)$$

where  $\sigma_{1s}^+$  is given by Eq. (1). The factor 2 accounts for two  $K$ -shell electrons in the target. Formula (2) holds for nonrelativistic atomic systems with nuclear charge  $Z \gg 1$ . In the following, we shall calculate the dominant correction with respect to the correlation parameter  $1/Z$ , which generalizes Eq. (2) for the case of small values of  $Z \gtrsim 2$ .

## II. FORMULATION OF PROBLEM

Let us assume that the incident electron has asymptotic momentum  $\mathbf{p}$  and energy  $E_p = p^2/(2m)$ , while the scattered electron is characterized by asymptotic momentum  $\mathbf{p}_1$  and energy  $E_{p_1} = p_1^2/(2m)$ . If  $p \gg \eta$  holds, the continuum wave function is approximated as  $\psi_p(\mathbf{r}) \simeq e^{i(\mathbf{p}\cdot\mathbf{r})}$  (Born approximation). The total ionization cross section is known to result mainly from the kinematics, where the asymptotic momentum of ejected electron is estimated as  $p_2 \sim \eta$ , but  $p_1 \sim p \gg \eta$  and, correspondingly,  $\psi_{p_1}(\mathbf{r}) \simeq e^{i(\mathbf{p}_1\cdot\mathbf{r})}$ . Then the interaction of the fast projectile with an atomic electron can be represented as the following potential:

$$U(\mathbf{r}) = \int \psi_{p_1}^*(\mathbf{r}')V(\mathbf{r},\mathbf{r}')\psi_p(\mathbf{r}')d\mathbf{r}' = D(\mathbf{q})e^{i(\mathbf{q}\cdot\mathbf{r})}. \quad (3)$$

Here  $V(\mathbf{r},\mathbf{r}') = \alpha/|\mathbf{r} - \mathbf{r}'|$  is the operator of the electron-electron Coulomb interaction,  $D(\mathbf{q}) = 4\pi\alpha/q^2$ , and  $\mathbf{q} = \mathbf{p} - \mathbf{p}_1$  is the recoil momentum transferred to the atom. In fact, Eq. (3) is valid only if the exchange interaction between the projectile and atomic electron can be neglected. In the case of high-energy electron scattering, such an interaction is associated with large momentum transfer and is suppressed by a factor of  $\sim(\eta/p)^2$  in the amplitude of the process.

In the Born approximation, the total amplitude for single ionization of a two-electron atom reads

$$\mathcal{A} = 2 \langle \Psi_f | U | \Psi_i \rangle, \quad (4)$$

where  $\Psi_{i,f}(\mathbf{r}_1,\mathbf{r}_2)$  are the two-electron wave functions of the initial and final states, respectively. The factor 2 takes into account the single-particle property of operator (3) and the symmetry of the wave functions. That is, it is sufficient to consider the interaction of the projectile with a single atomic electron only.

In the following, we shall take into account the Coulomb interaction between atomic electrons (correlations) in the initial and final atomic states. To zeroth-order approximation with respect to the correlation interaction, the wave functions  $\Psi_{i,f} \simeq \Psi_{i,f}^{(0)}$  are given by products of single-particle wave functions in the Coulomb field of the nucleus. For a heliumlike ion in the ground state, we have

$$\Psi_i^{(0)}(\mathbf{r}_1,\mathbf{r}_2) = \psi_{1s}(\mathbf{r}_1)\psi_{1s}(\mathbf{r}_2), \quad (5)$$

$$\Psi_f^{(0)}(\mathbf{r}_1,\mathbf{r}_2) = \frac{1}{\sqrt{2}} [\psi_{p_2}(\mathbf{r}_1)\psi_{1s}(\mathbf{r}_2) + \psi_{1s}(\mathbf{r}_1)\psi_{p_2}(\mathbf{r}_2)]. \quad (6)$$

The explicit expressions for the single-electron Coulomb wave functions read [22]

$$\psi_{1s}(\mathbf{r}) = N_{1s} e^{-\eta r}, \quad (7)$$

$$\psi_{p_2}(\mathbf{r}) = N_{p_2} e^{i(\mathbf{p}_2\cdot\mathbf{r})} F(-i\xi_2, 1, -i\rho_2), \quad (8)$$

where  $N_{1s}^2 = \eta^3/\pi$ ,  $N_{p_2}^2 = 2\pi\xi_2/(1 - e^{-2\pi\xi_2})$ ,  $\rho_2 = p_2 r + (\mathbf{p}_2 \cdot \mathbf{r})$ ,  $\xi_2 = \eta/p_2$ ,  $\eta = m\alpha Z$  is the characteristic momentum of a  $K$ -shell electron, and  $F(a,b,z)$  is the regular confluent hypergeometric function. Function (8) describes the continuum state, in which at infinity there are a plane wave and an incoming spherical one. Note, however, that due to the complex conjugation, the ionization amplitude contains the outgoing spherical waves.

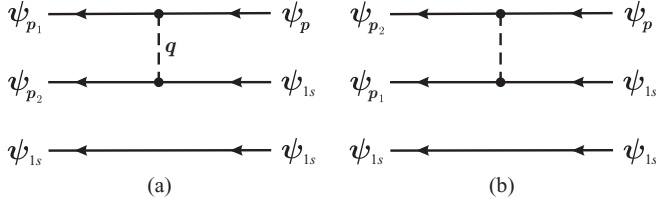


FIG. 2. Feynman diagrams describing the single ionization of a heliumlike ion to zeroth-order approximation with respect to the correlation interaction.

Equation (4) is given by

$$\mathcal{A} \simeq \mathcal{A}^{(0)} = 2\langle \Psi_f^{(0)} | U | \Psi_i^{(0)} \rangle = \sqrt{2} \langle \psi_{p_2} | U | \psi_{1s} \rangle. \quad (9)$$

The ionization amplitude (9) can be represented by the Feynman diagram depicted in Fig. 2(a) and has been thoroughly investigated in the literature [21–24]. In explicit form, it reads

$$\mathcal{A}^{(0)} = \sqrt{2} 16\pi\eta N_{1s} N_{p_2} D(\mathbf{q}) M_0, \quad (10)$$

$$M_0 = [q^2 - (1 + i\xi_2)(\mathbf{p}_2 \cdot \mathbf{q})] \frac{[(\mathbf{p}_2 - \mathbf{q})^2 + \eta^2]^{i\xi_2 - 2}}{[q^2 - (\mathbf{p}_2 + i\eta)^2]^{i\xi_2 + 1}}. \quad (11)$$

The exchange diagram, which is given by Fig. 2(b), is of minor importance in the case of high-energy electron scattering.

In order to get the universal scaling, we make the following substitutions:  $q \rightarrow \varkappa = q/\eta$ ,  $p_2 \rightarrow \xi_2^{-1} = p_2/\eta = \sqrt{\varepsilon_2}$ ,  $E_p \rightarrow \varepsilon = E_p/I$ , and  $E_{p_l} \rightarrow \varepsilon_l = E_{p_l}/I$  ( $l = 1, 2$ ). Then the energy-conservation law reads  $\varepsilon - 1 = \varepsilon_1 + \varepsilon_2$ . Formula (10) results in cross section (2) with the universal function  $\mathcal{Q}_{1s}(\varepsilon)$ , which is given by

$$\mathcal{Q}_{1s}(\varepsilon) = \frac{2^9}{\varepsilon} \int_0^{(\varepsilon-1)/2} \frac{d\varepsilon_2}{1 - e^{-2\pi\xi_2}} \int_{\varkappa_1}^{\varkappa_2} \frac{d\varkappa}{\varkappa^3} \int_0^\pi d\theta \sin\theta |\mathcal{M}_0|^2. \quad (12)$$

The dimensionless function  $\mathcal{M}_0$  is related to Eq. (11) by  $M_0 = \eta^{-4} \mathcal{M}_0$ . The limits of integration over the dimensionless momentum transfer  $\varkappa$  are defined according to  $\varkappa_1 = q_{\min}/\eta = (1 + \varepsilon_2)/\varkappa_2$  and  $\varkappa_2 = q_{\max}/\eta = \sqrt{\varepsilon} + \sqrt{\varepsilon - \varepsilon_2 - 1}$ , where  $q_{\min} = p - p_1$  and  $q_{\max} = p + p_1$ . The integration over the angle  $\theta$  between the momenta  $\mathbf{p}_2$  and  $\mathbf{q}$  can be performed analytically (see, for example, Refs. [21–24]):

$$\int_0^\pi d\theta \sin\theta |\mathcal{M}_0|^2 = \frac{2\varkappa^2}{3w^3} (3\varkappa^2 + 1 + \varepsilon_2) e^{-\varphi}, \quad (13)$$

$$w = (\varkappa^2 + 1 - \varepsilon_2)^2 + 4\varepsilon_2, \quad \varphi = \frac{2}{\sqrt{\varepsilon_2}} \cot^{-1} \left\{ \frac{\varkappa^2 + 1 - \varepsilon_2}{2\sqrt{\varepsilon_2}} \right\}. \quad (14)$$

The range of the principal value of  $\cot^{-1}(z)$  lies between 0 and  $\pi$ .

Now we shall construct the wave functions  $\Psi_{i,f}$  within the framework of the first-order perturbation theory with respect to the correlation interaction, namely,  $\Psi_{i,f} = \Psi_{i,f}^{(0)} + \Psi_{i,f}^{(1)}$ . The first-order corrections to the wave functions are found from the following equations [26,27]:

$$\Psi_i^{(1)} = (E_i^{(0)} - H_1 - H_2)^{-1} (1 - \mathcal{P}_i) V \Psi_i^{(0)}, \quad (15)$$

$$\Psi_f^{(1)} = (E_f^{(0)} - H_1 - H_2 + i0)^{-1} V \Psi_f^{(0)}. \quad (16)$$

Here  $E_i^{(0)} = 2E_{1s}$ , with  $E_{1s}$  being the single-electron energies in the initial bound state described by  $\Psi_i^{(0)}$ ,  $\mathcal{P}_i = |\Psi_i^{(0)}\rangle\langle\Psi_i^{(0)}|$  is the projection operator on this state,  $H_1$  and  $H_2$  are the single-particle Hamiltonians for an electron in the Coulomb field of the nucleus, and  $E_f^{(0)} = E_{1s} + E_{p_2}$ , where  $E_{p_2} = p_2^2/(2m)$  is the energy of the escaping electron.

The ionization amplitude is refined as follows:  $\mathcal{A} = \mathcal{A}^{(0)} + \mathcal{A}^{(1)}$ . The first-order corrections are given by

$$\begin{aligned} \mathcal{A}^{(1)} &= 2\langle \Psi_f^{(0)} | U | \Psi_i^{(1)} \rangle + 2\langle \Psi_f^{(1)} | U | \Psi_i^{(0)} \rangle \\ &= \sqrt{2} [\mathcal{A}_a + \mathcal{A}_b + \mathcal{A}_c + \mathcal{A}_d], \end{aligned} \quad (17)$$

where

$$\mathcal{A}_a = \langle \psi_{p_2} \psi_{1s} | U G_R(E_{1s}) V | \psi_{1s} \psi_{1s} \rangle, \quad (18)$$

$$\mathcal{A}_b = \langle \psi_{p_2} \psi_{1s} | V G(E_{p_2}) U | \psi_{1s} \psi_{1s} \rangle, \quad (19)$$

$$\mathcal{A}_c = \langle \psi_{1s} \psi_{p_2} | U G(E_c) V | \psi_{1s} \psi_{1s} \rangle, \quad (20)$$

$$\mathcal{A}_d = \langle \psi_{1s} \psi_{p_2} | V G(E_{p_2}) U | \psi_{1s} \psi_{1s} \rangle. \quad (21)$$

Here  $G(E) = (E - H_1)^{-1}$  denotes the single-particle Coulomb Green's function with energy  $E$ . The reduced Green's function  $G_R(E_{1s})$ , corresponding to energy  $E_{1s}$  of the  $K$ -shell electron, is given by

$$G_R(E_{1s}) = \lim_{E' \rightarrow E_{1s}} \left\{ G(E') - \frac{|\psi_{1s}\rangle\langle\psi_{1s}|}{E' - E_{1s}} \right\}. \quad (22)$$

In Eq. (20), the intermediate energy is defined as follows:  $E_c = 2E_{1s} - E_{p_2}$ . The amplitudes (18)–(21) can be presented by the Feynman diagrams depicted in Figs. 3(a)–3(d), respectively. Figures 3(a) and 3(c) describe the interaction between atomic electrons in the initial state, while Figs. 3(b) and 3(d) account for the interaction in the final state. The corresponding contributions are evaluated analytically in Sec. III.

It should be noted that Figs. 3(a)–3(d) can be considered as the diagrams which account for the interelectron interaction in the three-electron system up to second-order perturbation theory. Then there are also the additional Feynman diagrams, which take into account the twofold interaction of the projectile with atomic electrons [see Figs. 3(e)–3(g)]. However, the contribution of these diagrams is suppressed since the Green's function for the ionizing particle involves high energy. The corresponding estimate is made in Sec. III D.

### III. EVALUATION OF AMPLITUDES

#### A. Amplitude $\mathcal{A}_a$

In the following, we shall evaluate the matrix elements in the momentum representation. Then the operators  $U$  and  $V$  correspond to the photon propagators  $D(\mathbf{q}) = 4\pi\alpha/q^2$  and  $D(\mathbf{f}) = 4\pi\alpha/f^2$ , respectively, where  $\mathbf{q}$  is the momentum transferred to the atomic electron by the projectile, while  $\mathbf{f}$  is the exchange momentum of the atomic electrons interacting with each other. The analytical expression for matrix

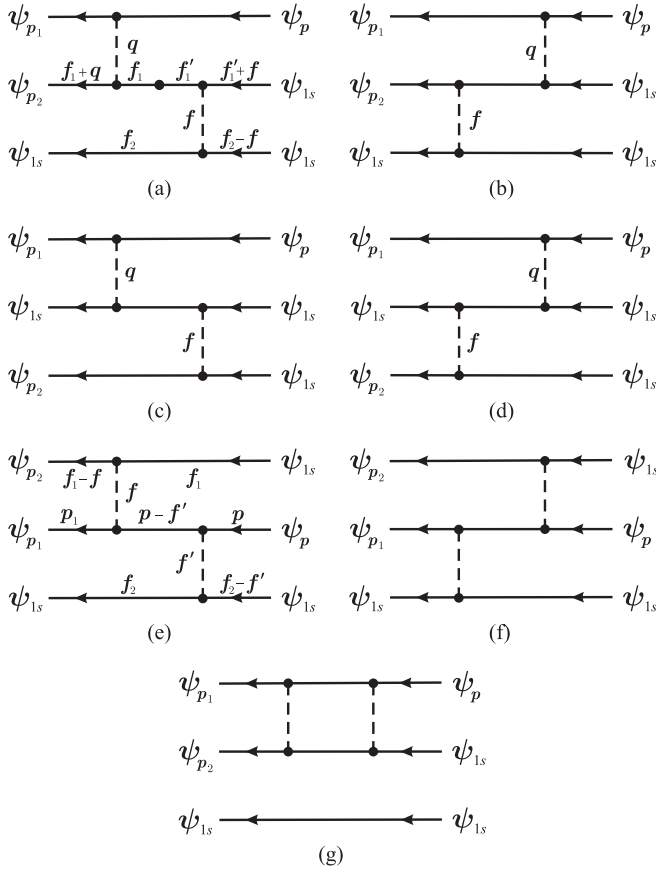


FIG. 3. Feynman diagrams describing the single ionization of a heliumlike ion by high-energy electron impact to next-to-leading order of the perturbation theory. In (a), the electron propagator with dot corresponds to the reduced Coulomb Green's function.

element (18) is given by

$$\mathcal{A}_a = D(\mathbf{q}) \int \langle \psi_{p_2} | \mathbf{f}_1 + \mathbf{q} \rangle \langle \mathbf{f}_1 | G_R(E_{1s}) | \mathbf{f}'_1 \rangle \langle \mathbf{f}'_1 + \mathbf{f} | \psi_{1s} \rangle \times F(\mathbf{f}) D(\mathbf{f}) \frac{d\mathbf{f}_1}{(2\pi)^3} \frac{d\mathbf{f}'_1}{(2\pi)^3} \frac{d\mathbf{f}}{(2\pi)^3}, \quad (23)$$

$$F(\mathbf{f}) = \int \langle \psi_{1s} | \mathbf{f}_2 \rangle \langle \mathbf{f}_2 - \mathbf{f} | \psi_{1s} \rangle \frac{d\mathbf{f}_2}{(2\pi)^3}. \quad (24)$$

In the momentum representation, the single-electron Coulomb wave functions can be expressed as follows [28,29]:

$$\langle \mathbf{f}_2 - \mathbf{f} | \psi_{1s} \rangle = N_{1s} \left( -\frac{\partial}{\partial \eta} \right) \langle \mathbf{f}_2 | V_{i\eta} | \mathbf{f} \rangle, \quad (25)$$

$$\langle \psi_{p_2} | \mathbf{f}_1 + \mathbf{q} \rangle = N_{p_2} \left( -\frac{\partial}{\partial v} \right) \hat{\mathcal{I}}_t \langle \mathbf{k} | V_{i\chi} | \mathbf{f}_1 \rangle_{|v \rightarrow 0}, \quad (26)$$

$$\hat{\mathcal{I}}_t = \frac{1}{2\pi i} \oint^{(0^+, 1^+)} \frac{dt}{t} \left( \frac{-t}{1-t} \right)^{i\xi_2}, \quad (27)$$

where  $\mathbf{k} = \mathbf{p}_2(1-t) - \mathbf{q}$ ,  $i\chi = p_2 t + i v$ , and  $\xi_2 = \eta/p_2$ . The integration contour in integral operator (27) is a closed curve enclosing once counterclockwise the points 0 and 1. After taking the derivative in Eq. (26), parameter  $v$  should tend to zero. In Eqs. (25) and (26), the matrix elements are defined by

$$\langle \mathbf{f}' | V_{i\mu} | \mathbf{f} \rangle = \frac{4\pi}{(\mathbf{f}' - \mathbf{f})^2 + \mu^2}. \quad (28)$$

Inserting expressions (25) and (26) into Eqs. (23) and (24), one obtains

$$\mathcal{A}_a = N_{1s} N_{p_2} D(\mathbf{q}) \frac{\partial^2}{\partial \eta \partial v} \hat{\mathcal{I}}_t \int F(\mathbf{f}) D(\mathbf{f}) \times \langle \mathbf{k} | V_{i\chi} G_R(E_{1s}) V_{i\eta} | -\mathbf{f} \rangle \frac{d\mathbf{f}}{(2\pi)^3}, \quad (29)$$

$$F(\mathbf{f}) = N_{1s}^2 \left( -\frac{\partial}{\partial \mu} \right) \langle \mathbf{f} | V_{i\mu} | 0 \rangle_{|\mu=2\eta}. \quad (30)$$

In Eq. (30), after taking derivative over  $\mu$ , one should set  $\mu = 2\eta$ . Using the operator identity

$$-\frac{\partial}{\partial \mu} V_{i\mu} V_{i\eta} = -\frac{\partial}{\partial \eta} V_{i\mu} V_{i\eta} = V_{i(\mu+\eta)}, \quad (31)$$

one can perform the integration over the intermediate momentum  $\mathbf{f}$  in Eq. (29). Then we have

$$\mathcal{A}_a = N_{1s}^3 N_{p_2} \frac{(4\pi\alpha)^2}{q^2} \frac{\partial^2}{\partial \mu \partial v} \frac{1}{\mu^2} [J(\eta) - J(\mu + \eta)], \quad (32)$$

$$J(\beta) = \hat{\mathcal{I}}_t \langle \mathbf{k} | V_{i\chi} G_R(E_{1s}) V_{i\beta} | 0 \rangle. \quad (33)$$

Equation (33) can be evaluated by using the method suggested in Refs. [30,31]. The general expression for the matrix element, which involves the Coulomb Green's function, is given by

$$\langle \mathbf{k}_2 | V_{i\eta_2} G(E) V_{i\eta_1} | \mathbf{k}_1 \rangle = -im \int_0^1 \frac{dx}{\Lambda} (\exp) \langle \mathbf{k}_2 | V_{\Lambda+i\eta_2} | \mathbf{k}_1 x \rangle, \quad (34)$$

$$\Lambda = \sqrt{(p^2 - k_1^2 x)(1-x) - \eta_1^2 x}, \quad (35)$$

$$(\exp) = \exp \left\{ i\eta \int_x^1 \frac{dx}{x\Lambda} \right\} = \left( \frac{k_1 + i\eta_1 - p k_1 x + \Lambda + p}{k_1 + i\eta_1 + p k_1 x + \Lambda - p} \right)^{i\xi}, \quad (36)$$

where  $p = \sqrt{2mE + i0}$  and  $\xi = \eta/p$ .

By virtue of Eqs. (22) and (34), the first part of matrix element (33) containing the Coulomb Green's function can be written as follows:

$$\langle \mathbf{k} | V_{i\chi} G(E') V_{i\beta} | 0 \rangle = -m \int_0^1 \frac{dx}{\Lambda_1} (\exp)_1 \langle \mathbf{k} | V_{i(\chi+\Lambda_1)} | 0 \rangle, \quad (37)$$

$$\Lambda_1 = \sqrt{p^2(1-x) + \beta^2 x}, \quad (38)$$

$$(\exp)_1 = \exp \left\{ \eta \int_x^1 \frac{dx}{x\Lambda_1} \right\} = x^{-\zeta} \left( \frac{\Lambda_1 + p'}{\beta + p'} \right)^{2\zeta}, \quad (39)$$

where  $p' = \sqrt{2m|E'|}$  and  $\zeta = \eta/p'$ . The second part of matrix element (33), which corresponds to the contribution due to the counterterm in Eq. (22), reads

$$\frac{\langle \mathbf{k} | V_{i\chi} | \psi_{1s} \rangle \langle \psi_{1s} | V_{i\beta} | 0 \rangle}{E' - E_{1s}} = -4\pi N_{1s}^2 \frac{\langle \mathbf{k} | V_{i(\chi+\eta)} | 0 \rangle}{(\beta + \eta)^2 \Delta}, \quad (40)$$

where the infinitesimally small shift  $\Delta = E_{1s} - E'$  is assumed to be positive.

Since the dependence on the variable  $t$  appears in  $\mathbf{k}$  and  $\chi$  only, the contour integral in Eq. (33) can be taken by using the



residue theorem. It yields

$$J(\beta) = 4\pi \lim_{\Delta \rightarrow +0} \left\{ -m \int_0^1 \frac{dx}{\Lambda_1} (\exp)_1 \Phi(\Lambda_1) + \frac{4\eta^3 \Phi(\eta)}{(\beta + \eta)^2 \Delta} \right\}, \quad (41)$$

$$\Phi(z) = \frac{[(q - p_2)^2 + (z + \nu)^2]^{i\xi_2 - 1}}{[q^2 + (z + \nu - ip_2)^2]^{i\xi_2}}. \quad (42)$$

Now we introduce the dimensionless parameter  $\delta = \Delta/(2I)$ , where  $I = \eta^2/(2m)$  is the binding energy of the  $K$ -shell electron. For simplicity, we also redefine Eq. (41) according to the relation  $J(\beta) = 4\pi m \mathcal{J}(\beta)$ . Then we obtain

$$\mathcal{J}(\beta) = \lim_{\delta \rightarrow 0} \left\{ - \int_0^1 x^{-\zeta} f(x) dx + \frac{4\eta \Phi(\eta)}{(\beta + \eta)^2 \delta} \right\}, \quad (43)$$

$$f(x) = \frac{1}{\Lambda_1} \left( \frac{\Lambda_1 + p'}{\beta + p'} \right)^{2\zeta} \Phi(\Lambda_1), \quad (44)$$

where  $p' = \eta\sqrt{1 + 2\delta}$  and  $\zeta = 1/\sqrt{1 + 2\delta}$ . In Eq. (43), the integral term contains the pole singularity  $\sim 1/\delta$  and a finite contribution at  $\delta \rightarrow 0$ . Integrating over parts yields

$$\int_0^1 x^{-\zeta} f(x) dx = \frac{f(1)}{\rho} - \frac{1}{\rho} \int_0^1 x^\rho f'(x) dx \quad (45a)$$

$$= \frac{f(0)}{\rho} - \int_0^1 f'(x) \ln x dx. \quad (45b)$$

Here  $\rho = 1 - \zeta \simeq \delta(1 - 3\delta/2)$ , and the prime over  $f(x)$  denotes the derivative with respect to  $x$ . In Eq. (45b), the integral term remains finite at  $\delta \rightarrow 0$ . Accordingly, it is convenient to introduce the notation  $g(x)$  for the function  $f(x)$  at  $\delta = 0$ :

$$g(x) = \lim_{\delta \rightarrow 0} f(x) = \frac{1}{L} \left( \frac{L + \eta}{\beta + \eta} \right)^2 \Phi(L), \quad (46)$$

$$L = \sqrt{\eta^2(1 - x) + \beta^2 x}. \quad (47)$$

In the limit  $\delta \rightarrow 0$ , the term outside the integral takes the form

$$\frac{f(0)}{\rho} = \frac{\Phi(p')}{\rho p'} \left( \frac{2p'}{\beta + p'} \right)^{2\zeta} \rightarrow \left( \frac{1}{\delta} + \frac{3}{2} + 2u + 2w \right) g(0), \quad (48)$$

$$g(0) = \frac{4\eta \Phi(\eta)}{(\beta + \eta)^2}, \quad u = \frac{1}{2} \frac{\beta - \eta}{\beta + \eta} - \ln \frac{2\eta}{\beta + \eta}, \quad (49)$$

$$w = \frac{\eta(i\xi_2 - 1)\eta_1}{(q - p_2)^2 + \eta_1^2} - \frac{\eta\xi_2(p_2 + i\eta_1)}{q^2 - (p_2 + i\eta_1)^2}, \quad (50)$$

where  $\eta_1 = \eta + \nu$ . Substituting Eqs. (45b) and (48) into Eq. (43), one observes that the pole terms cancel each other. Accordingly, we arrive at the following expressions:

$$\mathcal{A}_a = \mathcal{N} \frac{\partial^2}{\partial \mu \partial \nu} \frac{1}{\mu^2} [\mathcal{J}(\eta) - \mathcal{J}(\mu + \eta)]_{|\mu=2\eta, \nu \rightarrow 0}, \quad (51)$$

$$\mathcal{J}(\beta) = - \left( \frac{3}{2} + 2u + 2w \right) g(0) + \int_0^1 g'(x) \ln x dx. \quad (52)$$

The normalization factor  $\mathcal{N}$  is equal to  $\mathcal{N} = (4\pi)^3 \alpha^2 m N_{1s}^3 N_{p_2} / q^2$ . After taking derivatives in Eq. (51),

one should set  $\mu = 2\eta$  and take the limit  $\nu \rightarrow 0$ . The function  $g'(x)$  denotes the derivative of Eq. (46) with respect to  $x$ .

## B. Amplitude $\mathcal{A}_b$

The amplitude  $\mathcal{A}_b$  accounts for the interaction between the atomic electrons (or, more precisely, between the bound  $K$ -shell electron and the slow ionized electron) in the final state and can be presented as follows:

$$\mathcal{A}_b = D(\mathbf{q}) \int \langle \psi_{p_2} | f_1 - f \rangle \langle f_1 | G(E_{p_2}) | f'_1 \rangle \langle f'_1 - \mathbf{q} | \psi_{1s} \rangle \times F(\mathbf{f}) D(\mathbf{f}) \frac{d\mathbf{f}_1}{(2\pi)^3} \frac{d\mathbf{f}'_1}{(2\pi)^3} \frac{d\mathbf{f}}{(2\pi)^3} \quad (53)$$

$$= N_{1s} D(\mathbf{q}) \left( -\frac{\partial}{\partial \tau} \right) \int \langle \psi_{p_2} | f_1 - f \rangle F(\mathbf{f}) D(\mathbf{f}) \times \langle f_1 | G(E_{p_2}) V_{i\tau} | \mathbf{q} \rangle \frac{d\mathbf{f}_1}{(2\pi)^3} \frac{d\mathbf{f}}{(2\pi)^3} \Big|_{\tau=\eta}, \quad (54)$$

where the function  $F(\mathbf{f})$  is defined by Eq. (24). Due to relation (30), we can write

$$\frac{1}{f^2} F(\mathbf{f}) = N_{1s}^2 \left( -\frac{\partial}{\partial \mu} \right) \frac{1}{\mu^2} \langle f | (V_{i\lambda} - V_{i\mu}) | 0 \rangle_{|\lambda \rightarrow 0, \mu=2\eta}. \quad (55)$$

Here we have introduced a screened Coulomb potential with a Yukawa shape. This is done in order to avoid ambiguities related to the infrared divergency, which appears in the series expansion of perturbation theory for the case of a continuous spectrum in the Coulomb field. However, it is well known that all logarithmically divergent terms are summed in ionization amplitude up to an overall singular phase factor such as  $\exp[i\xi_2 \ln(\lambda/2p_2)]$ , where  $\xi_2 = \eta/p_2$ , and therefore do not contribute to the cross section [32–36]. Substituting Eq. (55) into Eq. (54) yields

$$\mathcal{A}_b = \hat{\Gamma}_{\mu\tau} \int \langle \psi_{p_2} | f_1 - f \rangle \langle f | (V_{i\lambda} - V_{i\mu}) | 0 \rangle \times \langle f_1 | G(E_{p_2}) V_{i\tau} | \mathbf{q} \rangle \frac{d\mathbf{f}_1}{(2\pi)^3} \frac{d\mathbf{f}}{(2\pi)^3} \quad (56a)$$

$$= \hat{\Gamma}_{\mu\tau} \langle \psi_{p_2} | (V_{i\lambda} - V_{i\mu}) G(E_{p_2}) V_{i\tau} | \mathbf{q} \rangle, \quad (56b)$$

$$\hat{\Gamma}_{\mu\tau} = 4\pi \alpha N_{1s}^3 D(\mathbf{q}) \frac{\partial^2}{\partial \mu \partial \tau} \frac{1}{\mu^2}. \quad (57)$$

Here the derivatives should be evaluated at points  $\mu = 2\eta$  and  $\tau = \eta$ . The screening parameter  $\lambda$  is assumed to have an infinitesimally small value.

In Eq. (56b), the matrix element can be further transformed by using formula (34):

$$\langle \psi_{p_2} | V_{iz} G(E_{p_2}) V_{i\tau} | \mathbf{q} \rangle = -im \int_0^1 \frac{dx}{\Lambda} (\exp) \langle \psi_{p_2} | V_{\Lambda + iz} | \mathbf{q} x \rangle, \quad (58)$$

$$\Lambda = \sqrt{(p_2^2 - q^2 x)(1 - x) - \tau^2 x + i0}, \quad (59)$$

$$(\exp) = x^{-i\xi_2} \left( \frac{(qx)^2 - (p_2 + \Lambda)^2}{q^2 - (p_2 + i\tau)^2} \right)^{i\xi_2}, \quad (60)$$

where  $p_2 = \sqrt{2mE_{p_2}}$  and  $\xi_2 = \eta/p_2$ . The positive imaginary infinitesimally small addition in the expression for  $\Lambda$  fixes the appropriate branch of the multivalued function. In Eq. (58), the matrix element is evaluated by using the integral representation for wave function (26). Then we obtain

$$\langle \psi_{p_2} | V_{\Lambda+iz} | \mathbf{q}x \rangle = 4\pi N_{p_2} \Psi(z), \quad (61)$$

$$\Psi(z) = \frac{[(\mathbf{q}x - \mathbf{p}_2)^2 - (\Lambda + iz)^2]^{i\xi_2-1}}{[(qx)^2 - (p_2 + \Lambda + iz)^2]^{i\xi_2}}. \quad (62)$$

Substituting Eqs. (58) and (61) into Eq. (56b) yields

$$\begin{aligned} \mathcal{A}_b &= -i\mathcal{N} \frac{\partial^2}{\partial \mu \partial \tau} \frac{1}{\mu^2} \int_0^1 \frac{dx}{\Lambda} (\exp) [\Psi(\lambda) - \Psi(\mu)] \\ &= \mathcal{A}_b^I + \mathcal{A}_b^{II}, \end{aligned} \quad (63)$$

where the normalization factor  $\mathcal{N}$  is similar to that in Eq. (51). After taking the derivatives, one should set  $\mu = 2\eta$  and  $\tau = \eta$ . The second part of the amplitude,  $\mathcal{A}_b^{II}$ , does not depend on the screening parameter  $\lambda$  and is suitable for numerical calculations.

Let us consider the first integral in Eq. (63) in more detail. One can write

$$\mathcal{A}_b^I = -i\mathcal{N} \frac{\partial^2}{\partial \mu \partial \tau} \frac{1}{\mu^2} \mathcal{K}(\lambda) = \frac{i\mathcal{N}}{4\eta^3} \frac{\partial}{\partial \tau} \mathcal{K}(\lambda)_{\lambda \rightarrow 0, \tau = \eta}, \quad (64)$$

$$\begin{aligned} \mathcal{K}(\lambda) &= \int_0^1 \frac{dx}{\Lambda} (\exp) \Psi(\lambda) \\ &= \left\{ \int_0^v + \int_v^1 \right\} \frac{dx}{\Lambda} (\exp) \Psi(\lambda) = \sum_{l=1}^2 \mathcal{K}_l(v, \lambda). \end{aligned} \quad (65)$$

In Eq. (65), we have partitioned the interval of integration by a small quantity  $v$ , which is assumed to satisfy to the following inequality:  $\lambda \ll v \ll 1$ . Since the integral  $\mathcal{K}_1(v, \lambda)$  is divergent at the lower limit of integration at  $\lambda = 0$ , we keep the dependence on parameter  $\lambda$ . Then one obtains

$$\begin{aligned} \mathcal{K}_1(v, \lambda) &= \frac{\Phi(\tau)}{p_2} \int_0^v dx x^{-i\xi_2} (x - i\lambda\beta)^{i\xi_2-1} \\ &= \frac{\Phi(\tau)}{p_2} \left\{ \ln \frac{v}{\lambda\beta} + \psi(1) - \psi(1 - i\xi_2) + \frac{i\pi}{2} \right\}, \end{aligned} \quad (66)$$

where

$$\Phi(\tau) = \frac{a^{i\xi_2-1}(\tau)}{b^{i\xi_2}(\tau)}, \quad \beta = \frac{2p_2}{a(\tau)}, \quad (67)$$

$$a(\tau) = (\mathbf{q} - \mathbf{p}_2)^2 + \tau^2, \quad b(\tau) = q^2 - (p_2 + i\tau)^2. \quad (68)$$

Here  $\psi(z)$  is the digamma function,  $\psi(1) = -\gamma_E$ , and  $\gamma_E \simeq 0.5772$  is the Euler's constant. In Eq. (66), the leading terms with respect to the small parameter  $\lambda/v$  are taken into account.

In the integral  $\mathcal{K}_2(v, \lambda)$  one can set  $\lambda = 0$ . Thus we have

$$\begin{aligned} \mathcal{K}_2(v, 0) &= \int_v^1 \frac{dx}{\Lambda} (\exp) \Psi(0) = \Phi(\tau) \int_v^1 \frac{dx}{x\Lambda} \\ &= \frac{\Phi(\tau)}{p_2} \left\{ \ln \frac{4p_2^2}{vb(\tau)} - i\pi + O(v) \right\}. \end{aligned} \quad (69)$$

Due to Eqs. (66) and (69), formula (65) reads

$$\mathcal{K}(\lambda) = \frac{\Phi(\tau)}{p_2} \left\{ \ln \frac{2p_2}{\lambda} + \ln \frac{a(\tau)}{b(\tau)} + \psi(1) - \psi(1 - i\xi_2) - \frac{i\pi}{2} \right\}. \quad (70)$$

Taking the derivative over  $\tau$  at the point  $\tau = \eta$  yields

$$\begin{aligned} \mathcal{A}_b^I &= -M_0 \frac{\mathcal{N}}{\eta^3} \left\{ \frac{1}{2} \frac{(1 + i\xi_2)a(\eta) - i\xi_2 b(\eta)}{q^2 - (1 + i\xi_2)(\mathbf{p}_2 \cdot \mathbf{q})} \right. \\ &\quad \left. + i\xi_2 \left( \ln \frac{2p_2}{\lambda} + \ln \frac{a(\eta)}{b(\eta)} + \psi(1) - \psi(1 - i\xi_2) - \frac{i\pi}{2} \right) \right\}, \end{aligned} \quad (71)$$

where  $M_0$  is given by Eq. (11). As will be shown later, the logarithmic divergency over the screening parameter  $\lambda$  cancels out in the expression for the cross section.

### C. Amplitudes $\mathcal{A}_c$ and $\mathcal{A}_d$

The amplitudes  $\mathcal{A}_c$  and  $\mathcal{A}_d$ , which describe the contributions of the exchange diagrams, can be evaluated in a similar manner as that in the previous subsections. However, now the final expressions become more complicated. The results are represented in the form of twofold integrals:

$$\mathcal{A}_c = \frac{\mathcal{N}}{2} \frac{\partial^3}{\partial \tau \partial \mu \partial \nu} \int_0^1 \frac{dx}{\Lambda_2} (\exp)_2 \int_0^1 \frac{dy}{L_1} P_1, \quad (72)$$

$$\mathcal{A}_d = -\frac{\mathcal{N}}{2} \frac{\partial^3}{\partial \tau \partial \mu \partial \nu} \int_0^1 \frac{dx}{\Lambda} (\exp) \int_0^1 \frac{dy}{L_2} P_2. \quad (73)$$

Here

$$\Lambda_2 = \sqrt{(\gamma^2 + q^2 x)(1-x) + \mu^2 x}, \quad (74)$$

$$(\exp)_2 = x^{-\zeta_1} \left( \frac{(qx)^2 + (\gamma + \Lambda_2)^2}{q^2 + (\gamma + \mu)^2} \right)^{\zeta_1}, \quad (75)$$

$$L_1 = \sqrt{(qx)^2 y(1-y) + (\Lambda_2 + \nu)^2 y}, \quad (76)$$

$$P_1 = \frac{[(qxy - \mathbf{p}_2)^2 + (L_1 + \tau)^2]^{i\xi_2-1}}{[(qxy)^2 + (L_1 + \tau - ip_2)^2]^{i\xi_2}}, \quad (77)$$

$$L_2 = \sqrt{-(qx)^2 y(1-y) + (\Lambda + i\mu)^2 y}, \quad (78)$$

$$P_2 = \frac{[(qxy - \mathbf{p}_2)^2 - (L_2 + i\nu)^2]^{i\xi_2-1}}{[(qxy)^2 - (p_2 + L_2 + i\nu)^2]^{i\xi_2}}, \quad (79)$$

where  $\mathcal{N} = (4\pi)^3 \alpha^2 m N_{1s}^3 N_{p_2} / q^2$ ,  $\gamma = \sqrt{2m|E_c|}$ , and  $\zeta_1 = \eta/\gamma$ . The functions  $\Lambda$  and  $(\exp)$  are defined by Eqs. (59) and (60), respectively. After taking the derivatives with respect to  $\tau$ ,  $\mu$ , and  $\nu$ , one should set  $\tau = \mu = \nu = \eta$ . Equations (72) and (73) do not contain any singularities and are convenient for numerical calculations.

### D. Estimate for the contribution of diagrams with twofold interaction between projectile and atomic electrons

Let us estimate the contribution of the diagram in Fig. 3(e). The projectile is assumed to have a high energy  $E_p \gg I$  and a large momentum  $p \gg \eta$ . In this case, the ionizing electron can be described in the intermediate state by the free Green's

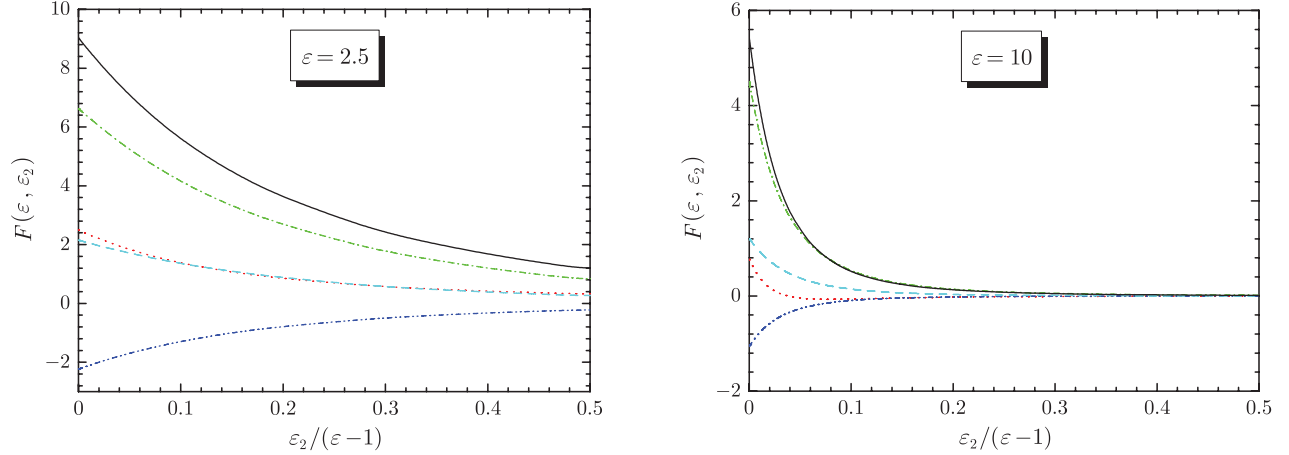


FIG. 4. (Color online) The energy distributions for different values of the dimensionless energy  $\varepsilon$  of the incident electron. Red dotted line, separate contribution of the Feynman diagram in Fig. 3(a); green dash-dotted line, contribution of the diagram in Fig. 3(b); blue dash-dot-dotted line, contribution of the diagram in Fig. 3(c); cyan dashed line, contribution of the diagram in Fig. 3(d); black solid line, total contribution of all diagrams.

function  $G_0(E_p)$  with an error of about  $\xi = \eta/p = \alpha Z/v$ . The analytic expression for the diagram in Fig. 3(e) is given by

$$\mathcal{A}_e = \int \Phi(\mathbf{f}) D(\mathbf{f}) G_0(\mathbf{p} - \mathbf{f}') D(\mathbf{f}') F(\mathbf{f}') \frac{d\mathbf{f}}{(2\pi)^3}, \quad (80)$$

$$\Phi(\mathbf{f}) = \int \langle \psi_{p_2} | \mathbf{f}_1 - \mathbf{f} \rangle \langle \mathbf{f}_1 | \psi_{1s} \rangle \frac{d\mathbf{f}_1}{(2\pi)^3}, \quad (81)$$

$$G_0(\mathbf{p} - \mathbf{f}') = \frac{2m}{p^2 - (\mathbf{p} - \mathbf{f}')^2 + i0} \simeq \frac{m}{(\mathbf{p} \cdot \mathbf{f}')^2} \sim \frac{1}{v\eta}, \quad (82)$$

where  $\mathbf{f}' = \mathbf{q} + \mathbf{f}$ . The function  $F(\mathbf{f}')$  is given by Eq. (24). Estimate (82) is obtained under the assumption that integral (80) is saturated at  $f \sim q \sim \eta$ .

Any one of the diagrams depicted in Figs. 3(a)–3(d) can be taken for comparison. We choose, for example, the diagram in Fig. 3(b), whose contribution to the amplitude of the ionization process is given by Eq. (53). Using the spectral expansion for

the Coulomb Green's function yields the following estimate:

$$\langle \mathbf{f}_1 | G(E_{p_2}) | \mathbf{f}'_1 \rangle \sim \frac{\langle \mathbf{f}_1 | \psi_{1s} \rangle \langle \psi_{1s} | \mathbf{f}'_1 \rangle}{E_{p_2} - E_{1s}}, \quad (83)$$

where  $E_{p_2} - E_{1s} \sim I$ . After substitution of Eq. (83) into Eq. (53), the integral over the intermediate momentum  $\mathbf{f}'_1$  yields

$$F(\mathbf{q}) = \frac{16\eta^4}{(q^2 + 4\eta^2)^2} \sim 1. \quad (84)$$

Then one can obtain

$$\mathcal{A}_b \sim \frac{1}{\alpha Z \eta} \int \Phi(\mathbf{f}) D(\mathbf{f}) F(\mathbf{f}) D(\mathbf{q}) \frac{d\mathbf{f}}{(2\pi)^3}. \quad (85)$$

Therefore, within the high-energy domain, the ratio of amplitudes is estimated according to

$$\frac{\mathcal{A}_e}{\mathcal{A}_b} \sim \frac{\alpha Z}{v} \ll 1. \quad (86)$$

#### IV. IONIZATION CROSS SECTION

The differential cross section for single  $K$ -shell ionization is related to the amplitude  $\mathcal{A} = \mathcal{A}^{(0)} + \mathcal{A}^{(1)}$  as follows:

$$d\sigma^+ = \frac{2\pi}{v} |\mathcal{A}|^2 \frac{d\mathbf{p}_1}{(2\pi)^3} \frac{d\mathbf{p}_2}{(2\pi)^3} \delta(E_{p_1} + E_{p_2} - E_p - E_{1s}) \quad (87a)$$

$$= 2d\sigma_{1s}^+ + d\sigma_{\text{cor}}^+. \quad (87b)$$

Equation (87a) defines the distributions over energy and ejection angles of the fast and slow electrons. The elements of phase volumes for the fast and slow electrons ejected into the solid angles  $d\Omega_1$  and  $d\Omega_2$ , respectively, can be written as

$$d\mathbf{p}_1 = m p_1 dE_{p_1} d\Omega_1 = 2\pi \frac{m}{p} dE_{p_1} q dq, \quad (88)$$

$$d\mathbf{p}_2 = m p_2 dE_{p_2} d\Omega_2 = 2\pi m p_2 dE_{p_2} \sin\theta d\theta, \quad (89)$$

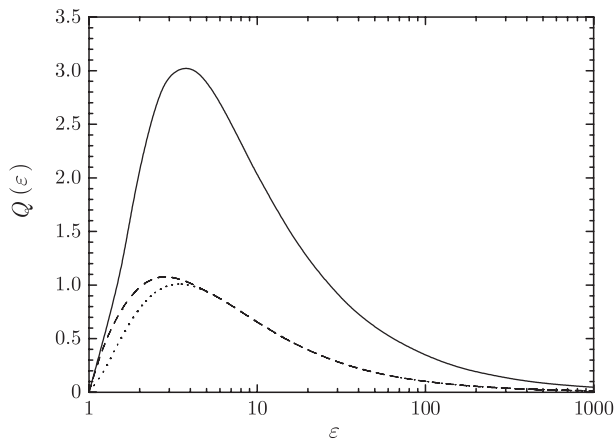


FIG. 5. The universal function  $Q(\varepsilon)$  vs the dimensionless energy  $\varepsilon$  (solid line). The single-electron universal function  $Q_{1s}(\varepsilon)$  is also given for comparison (dotted line, Born approximation; dashed line, calculation with the Coulomb wave functions).

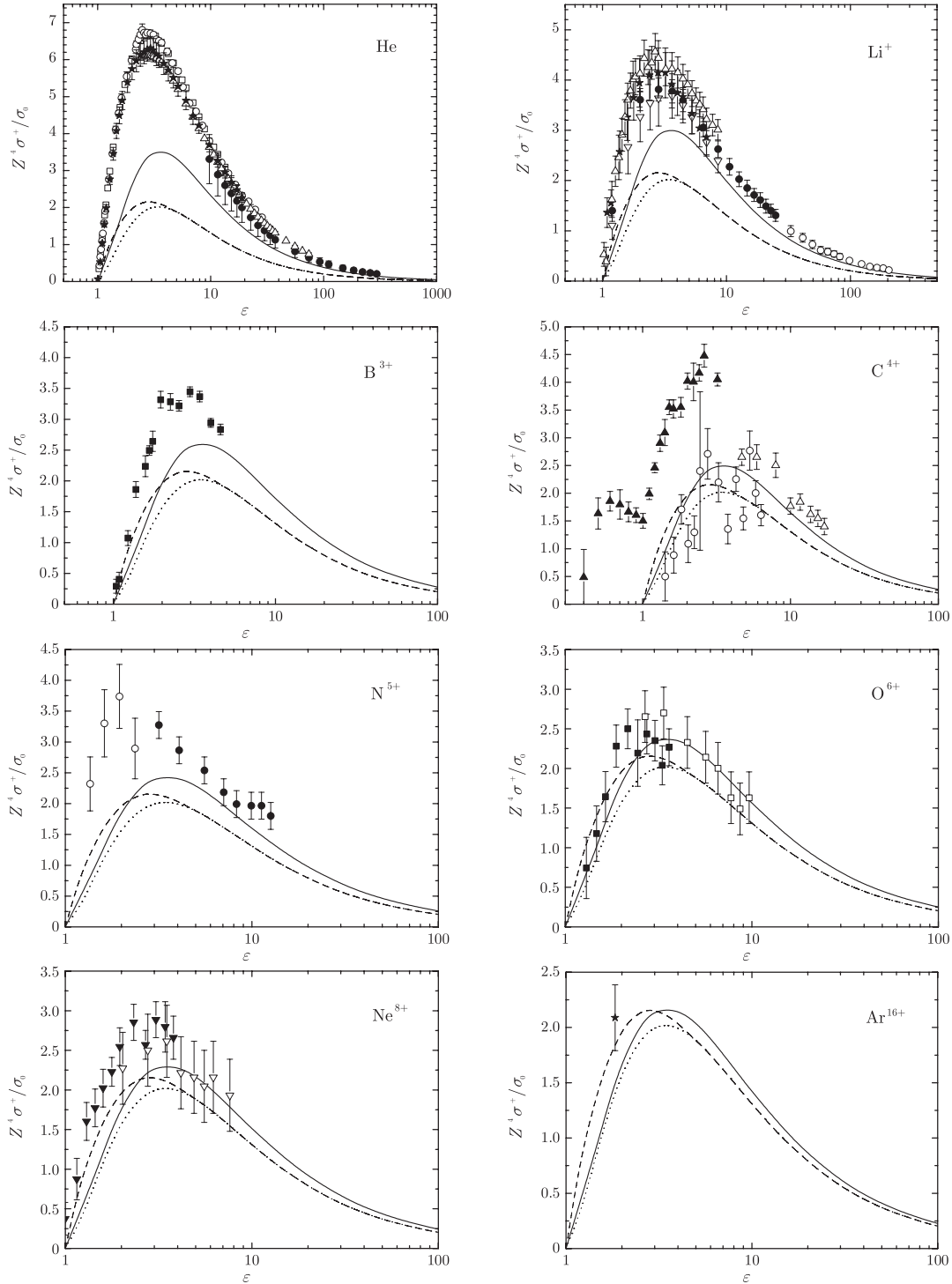


FIG. 6. A comparison between theoretical and experimental cross sections for the helium isoelectronic sequence. Perturbation theory to leading order: dotted line, Born approximation; dashed line, calculation with Coulomb wave functions. Perturbation theory, taking into account the dominant correlation contribution: solid line, Born approximation. Experimental data: for He, solid circles, [37]; squares, [38]; open circles, [39]; stars, [40]; triangles, [41]; for  $\text{Li}^+$ , stars, [42]; downward triangles, [43]; solid circles, [44]; open circles, [45]; upward triangles, [46]; for  $\text{B}^{3+}$ , squares, [47]; for  $\text{C}^{4+}$ , solid triangles, [47]; open triangles, [48]; open circles, [49]; for  $\text{N}^{5+}$ , open circles, [47]; solid circles, [48]; for  $\text{O}^{6+}$ , open squares, [48]; solid squares, [49]; for  $\text{Ne}^{8+}$ , open downward triangles, [48]; solid downward triangles, [50]; for  $\text{Ar}^{16+}$ , stars, [48].

where  $\theta$  is the angle between  $\mathbf{q}$  and  $\mathbf{p}_2$ . In Eq. (87b), the first term corresponds to the leading order of perturbation theory, while the second (interference) term describes the dominant correlation correction.

Let us now again introduce the dimensionless variables by the following substitution:  $q \rightarrow \varkappa = q/\eta$  and  $p_2 \rightarrow \xi_2^{-1} = p_2/\eta = \sqrt{\varepsilon_2}$ . Then the energy distribution for the correlation correction to the ionization cross section is



given by

$$\frac{d\sigma_{\text{cor}}^+}{d\varepsilon_2} = \frac{\sigma_0}{Z^5} F(\varepsilon, \varepsilon_2), \quad (90)$$

$$F(\varepsilon, \varepsilon_2) = \frac{2^{11}}{\varepsilon(1 - e^{-2\pi\varepsilon_2})} \int_{\varepsilon_1}^{\varepsilon_2} \frac{d\varkappa}{\varkappa^3} \int_0^\pi d\theta \sin\theta \text{Re}(\mathcal{M}_0^* \mathcal{M}_1), \quad (91)$$

where  $\sigma_0 = \pi a_0^2$ ,  $a_0 = 1/(m\alpha)$ , and the integration limits are the same as in Eq. (12). The dimensionless function  $\mathcal{M}_1$  is related to the amplitude [Eq. (17)] as follows:  $\mathcal{A}^{(1)} = \sqrt{2} \eta^{-7} \mathcal{N} \mathcal{M}_1$ . As easily seen from Eq. (91), due to the real part, the singular terms of the amplitude  $\mathcal{A}_b$  [see Eq. (71)] do not contribute to the cross section. The function  $F(\varepsilon, \varepsilon_2)$  does not depend explicitly on the particular value of  $Z$ .

Integrating Eq. (90) over the energy of ejected electrons yields

$$\sigma_{\text{cor}}^+ = \frac{\sigma_0}{Z^5} Q(\varepsilon), \quad (92)$$

$$Q(\varepsilon) = \int_0^{(\varepsilon-1)/2} F(\varepsilon, \varepsilon_2) d\varepsilon_2. \quad (93)$$

The function  $Q(\varepsilon)$  is universal. Finally, the total cross section for single  $K$ -shell ionization of heliumlike ions can be written as follows:

$$\sigma^+ = \frac{\sigma_0}{Z^4} \left( 2Q_{1s}(\varepsilon) + Q(\varepsilon) \frac{1}{Z} \right), \quad (94)$$

where the universal function  $Q_{1s}(\varepsilon)$  is given by Eq. (12). Formula (94), which is our main result, generalizes Eq. (2) to the case of light two-electron targets. Since the correlation correction simulates the screening effect, it improves significantly the theoretical predictions obtained within the framework of approximation of independent atomic electrons (noninteracting with each other).

## V. NUMERICAL RESULTS AND DISCUSSION

In Fig. 4, the energy distribution, Eq. (91), is presented for two values of the energy  $\varepsilon$  of incident electrons. Similar to the case of the leading order of perturbation theory, near the ionization threshold, the energy dependence is rather weak. Significant contributions to the cross section  $\sigma_{\text{cor}}^+$  arise from ejection of electrons with arbitrary energy sharing. At high energies  $\varepsilon \gg 1$ , the function  $F(\varepsilon, \varepsilon_2)$  becomes greatly nonuniform, being localized within the edge range of energies  $\varepsilon_2 \lesssim 1$ . The major correlation contribution to the ionization cross section is due to the amplitude  $\mathcal{A}_b$ , which accounts for the interaction between atomic electrons in the final state.

In Fig. 5, the universal function  $Q(\varepsilon)$  [Eq. (93)] is calculated versus the dimensionless energy  $\varepsilon$ , including the ionization threshold. Although the use of the Born approximation should be legitimate only within the asymptotic nonrelativistic range  $1 \ll \varepsilon \ll 2(\alpha Z)^{-2}$ , by analogy with the case of the leading order of perturbation theory (compare the dotted and dashed curves in Fig. 5), one can expect that proper accounting for the influence of the atomic nucleus on the wave functions of the

ionizing electron will not change significantly the magnitude of the next-to-leading-order correlation correction.

In Fig. 6, the theoretical function  $Z^4 \sigma^+ / \sigma_0$  is compared with available experimental data for the helium isoelectronic sequence with the nuclear charge  $Z$  within the range  $2 \leq Z \leq 18$ . Since in the lowest order of perturbation theory the Coulomb binding energies differ significantly from the ionization thresholds observed experimentally for targets with  $Z \gtrsim 2$ , we calibrate the incident electron energies  $E_p$  by the Coulomb ionization potential  $I$  but shift the experimental curve as a whole by the quantity  $1 - I_{\text{exp}}/I$  in order to fit the theoretical and experimental thresholds. This shift is crucial just within the near-threshold energy range, where our calculations are not accurate enough. The ionization potential  $I_{\text{exp}}$  is overadjusted by higher-order correlation corrections:

$$I_{\text{exp}} = I \left( \sum_{n \geq 0} \epsilon_n Z^{-n} - 1 \right), \quad (95)$$

where  $I = m(\alpha Z)^2/2$ ,  $\epsilon_0 = 2$ ,  $\epsilon_1 = -5/4$ ,  $\epsilon_2 = 0.3153$ , and  $\epsilon_3 = -0.0174$  [51]. Formula (95) reproduces the experimental thresholds for heliumlike targets with small values of  $Z \gtrsim 2$ . In general, the cross sections should be deduced at the same level of accuracy, taking into account higher-order terms of nonrelativistic perturbation theory. However, this problem is presently not solved. In the case of neutral helium, the significant deviation of experimental results from the theoretical prediction (94) is due to both the effect of the nuclear field on the wave functions of ionizing electron and the higher-order correlation corrections, which are neglected in this work. For heavier targets, the agreement between theory and experiment is quite satisfactory.

## VI. SUMMARY

We have deduced formulas for the dominant correlation correction to the single  $K$ -shell ionization cross sections of heliumlike ions by high-energy electron impact. The atomic targets are assumed to be characterized by the small parameters  $1/Z \ll 1$  and  $\alpha Z \ll 1$ . The study is performed by using nonrelativistic perturbation theory with respect to the interelectron interaction. The infrared divergency is isolated analytically in the ionization amplitude. The singularities are shown to cancel out in the expression for the cross section. The correlation correction appears mainly due to the interaction between atomic electrons in the final state. The ionizing electron is described within the framework of the Born approximation. Accordingly, the results obtained are also applicable for arbitrary charged projectiles, which are much lighter than the atomic nucleus. The cross section is represented in the form of universal scaling.

## ACKNOWLEDGMENTS

A.M. and A.N. are grateful to the Dresden University of Technology for hospitality. The authors also acknowledge financial support from the Max-Planck-Institut für Physik komplexer Systeme and from the RFBR under Grant No. 11-02-00943-a.

- [1] M. Inokuti, *Rev. Mod. Phys.* **43**, 297 (1971); M. Inokuti, Y. Itikawa, and J. E. Turner, *ibid.* **50**, 23 (1978).
- [2] C. J. Powell, *Rev. Mod. Phys.* **48**, 33 (1976).
- [3] M. E. Rudd, Y.-K. Kim, D. H. Madison, and J. W. Gallagher, *Rev. Mod. Phys.* **57**, 965 (1985).
- [4] H. Knudsen and J. F. Reading, *Phys. Rep.* **212**, 107 (1992).
- [5] K. P. Dere, *Astron. Astrophys.* **466**, 771 (2007).
- [6] M. Mattioli, G. Mazzitelli, M. Finkenthal, P. Mazzotta, K. B. Fournier, J. Kaastra, and M. E. Puiatti, *J. Phys. B* **40**, 3569 (2007).
- [7] A. Müller, *Adv. At. Mol. Opt. Phys.* **55**, 293 (2008).
- [8] L. B. Golden and D. H. Sampson, *J. Phys. B* **10**, 2229 (1977).
- [9] S. M. Younger, *J. Quantum Spectrosc. Radiat. Transfer* **26**, 329 (1981).
- [10] D. L. Moores and M. S. Pindzola, *Phys. Rev. A* **41**, 3603 (1990).
- [11] H. Deutsch, K. Becker, and T. D. Märk, *Int. J. Mass Spectrom. Ion Processes* **151**, 207 (1995).
- [12] C. J. Fontes, D. H. Sampson, and H. L. Zhang, *Phys. Rev. A* **59**, 1329 (1999).
- [13] C. R. Stia, O. A. Fojón, and R. D. Rivarola, *J. Phys. B* **33**, 1211 (2000).
- [14] H. Kolbenstvedt, *J. Appl. Phys.* **46**, 2771 (1975).
- [15] J. H. Scofield, *Phys. Rev. A* **18**, 963 (1978).
- [16] R. Anholt, *Phys. Rev. A* **19**, 1004 (1979).
- [17] P. Eschwey and P. Manakos, *Z. Phys. A* **308**, 199 (1982).
- [18] A. I. Mikhailov, A. V. Nefiodov, and G. Plunien, *Zh. Eksp. Teor. Fiz.* **136**, 885 (2009) [*JETP* **109**, 762 (2009)].
- [19] A. I. Mikhailov, A. V. Nefiodov, and G. Plunien, *Phys. Lett. A* **358**, 211 (2006).
- [20] A. I. Mikhailov, A. V. Nefiodov, and G. Plunien, *Phys. Lett. A* **368**, 391 (2007).
- [21] H. Bethe, *Ann. Phys.* **397**, 325 (1930).
- [22] L. D. Landau and E. M. Lifshitz, *Quantum Mechanics: Non-Relativistic Theory* (Pergamon, Oxford, 1991).
- [23] J. H. McGuire, *Electron Correlation Dynamics in Atomic Collisions* (Cambridge University Press, Cambridge, 1997).
- [24] A. I. Mikhailov, A. V. Nefiodov, and G. Plunien, *Phys. Lett. A* **372**, 4451 (2008).
- [25] M. B. Shah, D. S. Elliott, and H. B. Gilbody, *J. Phys. B* **20**, 3501 (1987).
- [26] E. J. Kelsey and J. Sucher, *Phys. Rev. A* **11**, 1829 (1975).
- [27] A. I. Mikhailov, I. A. Mikhailov, A. N. Moskalev, A. V. Nefiodov, G. Plunien, and G. Soff, *Phys. Rev. A* **69**, 032703 (2004).
- [28] H. A. Bethe and E. E. Salpeter, *Quantum Mechanics of One- and Two-Electron Atoms* (Plenum, New York, 1977).
- [29] V. G. Gorshkov, A. I. Mikhailov, and V. S. Polikanov, *Nucl. Phys.* **55**, 273 (1964).
- [30] V. G. Gorshkov, *Zh. Eksp. Teor. Fiz.* **47**, 352 (1964) [*Sov. Phys. JETP* **20**, 234 (1965)].
- [31] V. G. Gorshkov and V. S. Polikanov, *Pis'ma Zh. Eksp. Teor. Fiz.* **9**, 464 (1969) [*JETP Lett.* **9**, 279 (1969)].
- [32] V. G. Gorshkov, *Zh. Eksp. Teor. Fiz.* **40**, 1481 (1961) [*Sov. Phys. JETP* **13**, 1037 (1961)].
- [33] J. R. Taylor, *Nuovo Cimento B* **23**, 313 (1974).
- [34] J. McEnnan, L. Kissel, and R. H. Pratt, *Phys. Rev. A* **13**, 532 (1976); **13**, 2325 (1976).
- [35] M. Kolsrud, *J. Phys. A* **11**, 1271 (1978).
- [36] A. I. Mikhailov, *Zh. Eksp. Teor. Fiz.* **98**, 838 (1990) [*Sov. Phys. JETP* **71**, 465 (1990)].
- [37] B. L. Schram, A. J. H. Boerboom, and J. Kistemaker, *Physica* **32**, 185 (1966).
- [38] R. G. Montague, M. F. A. Harrison, and A. C. H. Smith, *J. Phys. B* **17**, 3295 (1984).
- [39] M. B. Shah, D. S. Elliott, P. McCallion, and H. B. Gilbody, *J. Phys. B* **21**, 2751 (1988).
- [40] R. Rejoub, B. G. Lindsay, and R. F. Stebbings, *Phys. Rev. A* **65**, 042713 (2002).
- [41] A. A. Sorokin, I. L. Beigman, S. V. Bobashev, M. Richter, and L. A. Vainshtein, *J. Phys. B* **37**, 3215 (2004).
- [42] W. C. Lineberger, J. W. Hooper, and E. W. McDaniel, *Phys. Rev.* **141**, 151 (1966).
- [43] J. B. Wareing and K. T. Dolder, *Proc. Phys. Soc.* **91**, 887 (1967).
- [44] B. Peart and K. T. Dolder, *J. Phys. B* **1**, 872 (1968).
- [45] B. Peart, D. S. Walton, and K. T. Dolder, *J. Phys. B* **2**, 1347 (1969).
- [46] A. Borovik, Jr., A. Müller, S. Schippers, I. Bray, and D. V. Fursa, *J. Phys. B* **42**, 025203 (2009).
- [47] D. H. Crandall, R. A. Phaneuf, and D. C. Gregory, Oak Ridge National Laboratory, Report No. ORNL/TM-7020, 1979 (unpublished); <http://www-cfadc.phy.ornl.gov/xbeam/index.html>
- [48] E. D. Donets and V. P. Ovsyannikov, *Zh. Eksp. Teor. Fiz.* **80**, 916 (1981) [*Sov. Phys. JETP* **53**, 466 (1981)].
- [49] S. Rachafi, M. Zambra, Z. Hui, M. Duponchelle, J. Jureta, and P. Defrance, *Phys. Scr. T* **28**, 12 (1989).
- [50] M. Duponchelle, M. Khouilid, E. M. Oualim, H. Zhang, and P. Defrance, *J. Phys. B* **30**, 729 (1997).
- [51] J. Mittdal, *Phys. Rev.* **138**, A1010 (1965).